PORTLAND PRESS

Research Article

Pathogenic role of human C-reactive protein in diabetic retinopathy

Fangfang Qiu[1,2,*], **Xiang Ma**[1,*], **Young-Hwa Shin**[1], **Jianglei Chen**[1], **Qian Chen**[1,3], **Kelu Zhou**[1], **Wenjing Wu**[1], **Wentao Liang**[1], **Yalin Wu**[3], **Qing Song**[4] **and** [ID] **Jian-Xing Ma**[1]

[1]Department of Physiology, University of Oklahoma Health Sciences Center, Oklahoma City, OK, U.S.A.; [2]Department of Ophthalmology, Tufts Medical Center, Boston, MA, U.S.A.; [3]Eye Institute of Xiamen University, Xiamen City, Fujian Province, China; [4]Cardiovascular Research Institute, Morehouse School of Medicine, Atlanta, GA, U.S.A.

Correspondence: Jian-Xing Ma (jian-xing-ma@ouhsc.edu) or Qing Song (qsong@msm.edu)

OPEN ACCESS

Purpose: Elevated blood levels of C-reactive protein (CRP) are associated with both type 1 and type 2 diabetes and diabetic complications, such as diabetic retinopathy (DR). However, its pathogenic role in DR remains unknown. The present study aims to investigate the potential role of CRP in DR pathogenesis and explore its underlying mechanism.
Materials and methods: Human CRP transgenic (hCRP-Tg) rats were employed for streptozotocin (STZ)-induced diabetic and oxygen-induced retinopathy (OIR) models. The retina function was monitored by electroretinography (ERG) and retinal thickness was measured by optical coherence tomography (OCT). TUNEL and cell death ELISA were performed to measure the apoptosis. Oxidative stress was detected by the measurement of reactive oxygen species (ROS) in cells and 3-Nitrotyrosine staining in tissue sections.
Results: In non-diabetic condition, hCRP-Tg with elevated hCRP levels in the retinas demonstrated declined ERG responses and decreased retinal thickness. In STZ-induced diabetic condition, overexpression of hCRP deteriorated retinal neurodegeneration as shown by ERG and apoptosis assays. hCRP also exacerbated retinal leukostasis and acellular capillary formation induced by diabetes. In the OIR model, overexpression of hCRP exacerbated retinal neovascularization (NV). In retinal cell lines, hCRP treatment induced cell death and over-production of ROS. Furthermore, hCRP-induced overexpression of pro-inflammatory, pro-oxidative, and pro-angiogenic factors was associated with up-regulation of CD32 and the NF-κB signaling in the retinas.
Conclusions: Elevated hCRP levels play a pathogenic role in DR. Targeting the hCRP-CD32-NF-κB pathway may represent a novel therapeutic strategy for DR.

Introduction

Diabetic retinopathy (DR) is the leading cause of vision loss in working-age people in developed countries [1]. Non-proliferative DR (NPDR) presents with progressive intra-retinal leukocyte adherence, retinal neuron degeneration, capillary degeneration, and retinal vascular leakage [2,3]. Without proper treatment, DR can progress to its advanced stage, proliferative DR (PDR), characterized by pathological angiogenesis in the retina [4]. Accumulating evidence demonstrated that impairment of the neurovascular unit due to elevated oxidative stress and inflammation in the retina plays a key role in DR [5–7].

C-reactive protein (CRP) is a prototypical acute-phase protein and predominantly expressed in hepatocytes in response to infection, inflammation, or tissue injury [8]. Previous studies showed that CRP is over-produced in both type 1 and type 2 diabetic patients [9,10]. Accumulating evidence suggests that high levels of CRP are associated with the risk of diabetic microvascular complications, such as nephropathy, neuropathy, and retinopathy [11–13]. At the baseline visit of the Diabetes Control and Complications Trial (DCCT), participants with DR showed significantly higher serum CRP levels compared with those without retinopathy [11]. Furthermore, another two studies demonstrated higher serum CRP levels in

patients with PDR compared with those with NPDR [12,13]. These epidemiological studies suggested that CRP can be used as a biomarker of diabetic complications. However, the underlying mechanism for the positive association between CRP and diabetic complications, especially DR, remains unknown.

It has been reported that CRP induces the generation of reactive oxygen species (ROS) and inflammation by binding with Fcγ receptors, including Fcγ receptor I (CD64) and Fcγ receptor II (CD32) [14–16]. CRP can activate the NF-κB signaling pathway, resulting in the generation of ROS and up-regulation of pro-inflammatory factors, such as tumor necrosis factor-α (TNF-α), and cell adhesion molecules, such as intercellular adhesion molecule-1 (ICAM-1) [17]. Liu et al. reported that elevated CRP levels in CRP transgenic mice promoted inflammation and fibrosis in the kidney in the context of diabetes [18]. Also, a recent study showed that CRP exerts a potent angiogenic effect on microvascular endothelial cells [19]. Furthermore, there is evidence that CRP plays a role in the apoptosis process [20]. While CRP has been indicated as the mediator of disease in non-ocular tissues, the pathogenic role of CRP in DR remains unknown.

In the present study, we tested the hypothesis that elevated levels of CRP may contribute to neurovascular impairment in DR by increasing retinal oxidative stress and inflammation. To investigate the pathogenic role of CRP in the context of DR, we used streptozotocin (STZ)-induced type 1 diabetic model in human CRP transgenic (hCRP-Tg) rats. To further investigate the role of CRP in retinal neovascularization (NV) and inflammation, we used the rat model of oxygen-induced retinopathy (OIR). We also measured the CRP-induced oxidative stress and apoptosis in immortalized rat retinal Müller cells (rMC-1) and mouse retinal precursor-like cells (661W) *in vitro*.

Methods
Animals
hCRP-Tg Sprague–Dawley rats were generated as described previously [21,22]. hCRP transgene was under the control of mouse albumin enhancer/promoter. The transgene construct of hCRP-Tg rats and genotyping of hCRP-Tg rats were described previously [21]. Wild-type (WT) littermate rats were used as control. All rats were housed in a specific pathogen-free (SPF) environment at 25°C under a 12-h/12-h light–dark cycle at animal facility of University of Oklahoma Health Sciences Center (OUHSC). In all procedures, rats were anesthetized with an intraperitoneal injection of ketamine–xylazine mix (K, 50 mg/kg; X, 5 mg/kg). All procedures using experimental animals were approved by the Institute Animal Care and Use Committee (IACUC) at the OUHSC, and all experiments were performed in compliance with the guidelines of the Association for Research in Vision and Ophthalmology (ARVO) Statement for the Use of Animals in Ophthalmic and Visual Research.

Induction of diabetes
Diabetes was induced in 2-month-old hCRP-Tg rats and WT Sprague–Dawley rats by an STZ injection (55 mg/kg body weight) as described previously [23]. Levels of blood glucose were monitored 3 days after the STZ injection and measured weekly thereafter. Rats with blood glucose constantly higher than 350 mg/dl were considered diabetes [23].

OIR model and quantification of retinal NV
OIR was generated as described previously [24]. Briefly, newborn pups were placed in an oxygen chamber with daily cycling of oxygen concentrations between 80 and 21% from the age postnatal days 0 (P0) to 13 (P13). The animals were maintained in the 12-h light and dark cycle at standard room temperature and humidity. At P14 and P18, fluorescein retinal angiography was performed to quantify the non-perfused area and NV, respectively. Another group of OIR animals were used for retinal histologic and Western blot analysis. Age-matched rats maintained at constant room air were used as normal controls.

Fundus imaging
WT and hCRP-Tg rats were anesthetized, and pupils were dilated with topical application of cyclopentolate (Akorn, Lake Forest, IL, U.S.A.). Fundus images were captured using Micron IV (Phoenix Research Laboratories, Pleasanton, CA, U.S.A.).

Electroretinography recording
Electroretinography (ERG) was recorded using the Espion Visual Electrophysiology System (Diagnosys, Lowell, MA). Rats were dark-adapted for 16 h for scotopic ERG. The full ERG responses of both eyes were simultaneously recorded at the flash intensity of 600 cd.s/m^2, and the data in both eyes were recorded and the average of left and right eyes were used for the analysis.

Optical coherence tomography

The retinal thickness was measured using a spectral-domain optical coherence tomography (SD-OCT) device (Biopti-gen Inc. Durham, NC) following a previously established method [23]. Images were captured with the rectangular scan at 1000 A-scans per B scan, and 200 B-scans per frame. Total retinal thickness was recorded and averaged at 3 × 3 grid positions, 500 μm from the center of the optic nerve head using the InVivo Vue driver software (Bioptigen). The researchers performing the OCT measurement were blinded to the animal group information.

Retinal leukostasis assay

Adherent leukocytes in the retinal vasculature were stained by perfusion with FITC-conjugated concanavalin-A (200 μg/ml), viewed in flat-mounted retinas, and quantified as described previously [25,26].

Retinal trypsin digestion

The eyeball was fixed in 4% paraformaldehyde in PBS solution for 3 days. The retina was dissected and digested with 5% trypsin for 1 h. Then, the retina vessels were gently isolated and stained with Periodic acid–Schiff staining system (Sigma–Aldrich, St. Louis, MO). Avascular capillaries in five random fields of each flat-mounted retinal vasculature were quantified according to a documented protocol [27].

Retinal vascular permeability assay

Retinal vascular permeability was measured according to the previous publications [28,29]. Briefly, Evans Blue (30 mg/ml) was carefully injected through the femoral vein (20 mg/kg body weight). Two hours after the Evans Blue injection, the rats were perfused via the left ventricle with pre-warmed PBS solution. Immediately after the perfusion, the retinas were harvested. Evans Blue dye in the retinas was extracted with formamide. The concentrations of Evans Blue in the extracts were measured and normalized by total retinal protein concentrations.

Western blot analysis

Western blot analysis was performed as described previously [30]. Antibodies for human CRP, TNF-α, total NF-κB p65, and CD64 were purchased from Abcam (Cambridge, MA). Antibodies for phosphorylated NF-κB p65 (Ser^{536}), phosphorylated IKKα/β (Ser$^{176/180}$), total IKKα, and total IKKβ were obtained from Cell Signaling (Danvers, MA). Antibodies for total β-catenin and anti-ICAM-1 were purchased from Santa Cruz Biotechnology (Santa Cruz, CA). An antibody for CD32 was obtained from R&D Systems (Minneapolis, MN). An antibody for β-actin was purchased from Sigma–Aldrich (St. Louis, MO). Details of primary and secondary antibodies used in the present study are shown in Supplementary Table S1.

Immunohistochemistry and TUNEL staining

For paraffin-embedded sections, rat eyeballs were enucleated and fixed in Davidson's fixative for 48 h. The eyeballs were embedded in paraffin and 5-μm sections were cut. The deparaffinization and antigen retrieval were performed as described previously [31]. The sections were immunostained with antibodies for 3-Nitrotyrosine (3-NT, Abcam, Cambridge, MA), CD32, human CRP, and rhodopsin (1D4, Abcam, Cambridge, MA). The eyeball sections were stained with peanut agglutinin (PNA; Vector Laboratories, Burlingame, CA) for labeling cone cells. For TUNEL staining, the section slides were incubated in TUNEL reaction mixture containing the enzyme and label solution for 1 h at 37°C in the dark according to the protocols of *In Situ* Cell Death Kit (Roche Molecular Biochemicals, Indianapolis, IN). In addition, the retina section treated with DNase1 was used as a positive control of TUNEL staining. The slides were mounted with mounting buffer containing DAPI (blue) and then photographed with a laser scanning confocal microscope (FV1000) (Olympus, PA, U.S.A.). For the quantification, the 3-NT intensity was measured by ImageJ software (Bethesda, MD, U.S.A.) according to a documented protocol [32]. Briefly, the whole area of retinal section was selected. Then, 'mean gray value' was measured in the selected areas. The values were normalized to the average value of non-diabetic WT rats. For counting TUNEL-positive cells or retinal neuronal cells, cells were counted in three random fields of the central regions (from immediately adjacent to the optic nerve to approximately 1000 μm from optic nerve) of both of the superior and inferior directions in each retinal section. In each group, a minimum of six retinal sections taken from six different rats were used for analysis.

Cell culture

The immortalized rMC-1 were kindly provided by Dr. Vijay Sarthy at Northwestern University, and cultured in Dulbecco's Modified Eagle's Medium (DMEM) containing 1 g/l glucose and 10% fetal bovine serum (FBS, Invitrogen,

Carlsbad, CA) [33]. The 661W cell line was a generous gift from Dr. Muayyad R. Al-Ubaidi at University of Houston, and cultured as described previously [34]. A human retinal pigment epithelia cell line (ARPE-19) was purchased from American Type Culture Collection (ATCC) and cultured in DMEM/F12 medium containing 1 g/l glucose and 10% FBS. For hCRP treatment, hCRP concentration of 10 µg/ml was selected according to previous publications [14,35–37].

Cell death ELISA
DNA fragmentation was measured in the retinal tissue and cell lines using the cell death ELISA kit (Roche Molecular Biochemicals, Indianapolis, IN) as described previously [25]. Histone-associated DNA fragments were measured at 405/490 nm absorbance. The relative readout was normalized by total protein concentration.

Cell viability assay
Cell viability was measured by Trypan Blue exclusion assay (Thermo Fisher, Grand Island, NY) as described previously [38]. Briefly, cell pellets were collected and re-suspended in PBS to reach the density of approximately 10^5–10^6/ml. Then, Trypan Blue dye solution was added into cell suspension at 1:1 ratio (v/v) to reach the final concentration of 0.2%. Viable and dead cells were quantified using the Cellometer (Nexcelom, Lawrence, MA).

Measurement of ROS
661W cells and rMC-1 cells were starved in serum-free DMEM for 16 h. The cells were then treated with 10 µg/ml hCRP for 3 h. Untreated cells and BSA-treated cells were served as control group. For hCRP treatment, the purified native CRP from human ascites (Sigma–Aldrich, St. Louis, MO) was used. The cells were incubated with fluorescent dye 2′,7′-dichlorodihydrofluorescein diacetate (H2DCFDA) (Invitrogen, Carlsbad, CA) for 30 min. Then, the DCF fluorescence signal was measured by the Wallac 1420 manager system.

Luciferase reporter assay
To measure β-catenin transcriptional activity, luciferase-based promoter assay was performed in rMC-1 cells and ARPE-19 cells as described previously [39]. Cells were transfected with 0.30 µg TOPFLASH plasmid containing the luciferase reporter gene under the control of a promoter containing β-catenin/TCF-binding sites and 0.20 µg pRL-TK plasmid for each well of the 24-well plate using Lipofectamine 2000. Then, cells were treated with 10 µg/ml hCRP for 16 h in the presence of 20% L cell conditioned medium or Wnt3A conditioned medium. Untreated cells and BSA-treated cells were used as control of hCRP-treated cells. Then, the cells were lysed for measuring luciferase activity using a dual luciferase assay kit (Promega, Madison, WI) following the Promega's protocol.

Statistics
Experiments were performed at least three times independently for *in vitro* experiments, and at least six rats per group were used for animal experiments. Results were presented as the mean $\pm$ standard error of the mean (SEM). Statistical analyses were performed using a two-tailed Student's *t* test for comparison of two groups, or using ANOVA followed by the Student–Newman–Keuls test when more than two groups were compared. $P < 0.05$ was set as statistically significant.

Results
Higher levels of CRP in the circulation of hCRP-Tg rats
As shown by Western blot analysis, hCRP was detected in the liver, kidney, heart, and retina of hCRP-Tg rats (Supplementary Figure S1A,B). Total serum hCRP levels in hCRP-Tg rats were 28.5 mg/l at 2 months of age, and increased to 38.7 mg/l at 5 months, and 43.9 mg/l by the end of 9 months, indicating that the transgene showed increasing expression with age (Supplementary Figure S1C). Moreover, these hCRP-Tg rats fed standard chow *ad libitum* showed normal levels of fasting blood glucose levels and slightly higher body weights as measured at 3 and 12 months of age compared with WT rats, suggesting that hCRP overexpression does not cause hyperglycemia in rats under normal conditions (Supplementary Figure S1D,E).

Impaired retinal function in hCRP-Tg rats
To examine retinal function, ERG analysis was performed on rats at the ages of 3, 6, and 9 months. The amplitudes of scotopic ERG response to a series of light intensity were shown in Supplementary Figure S2A,B. For recording
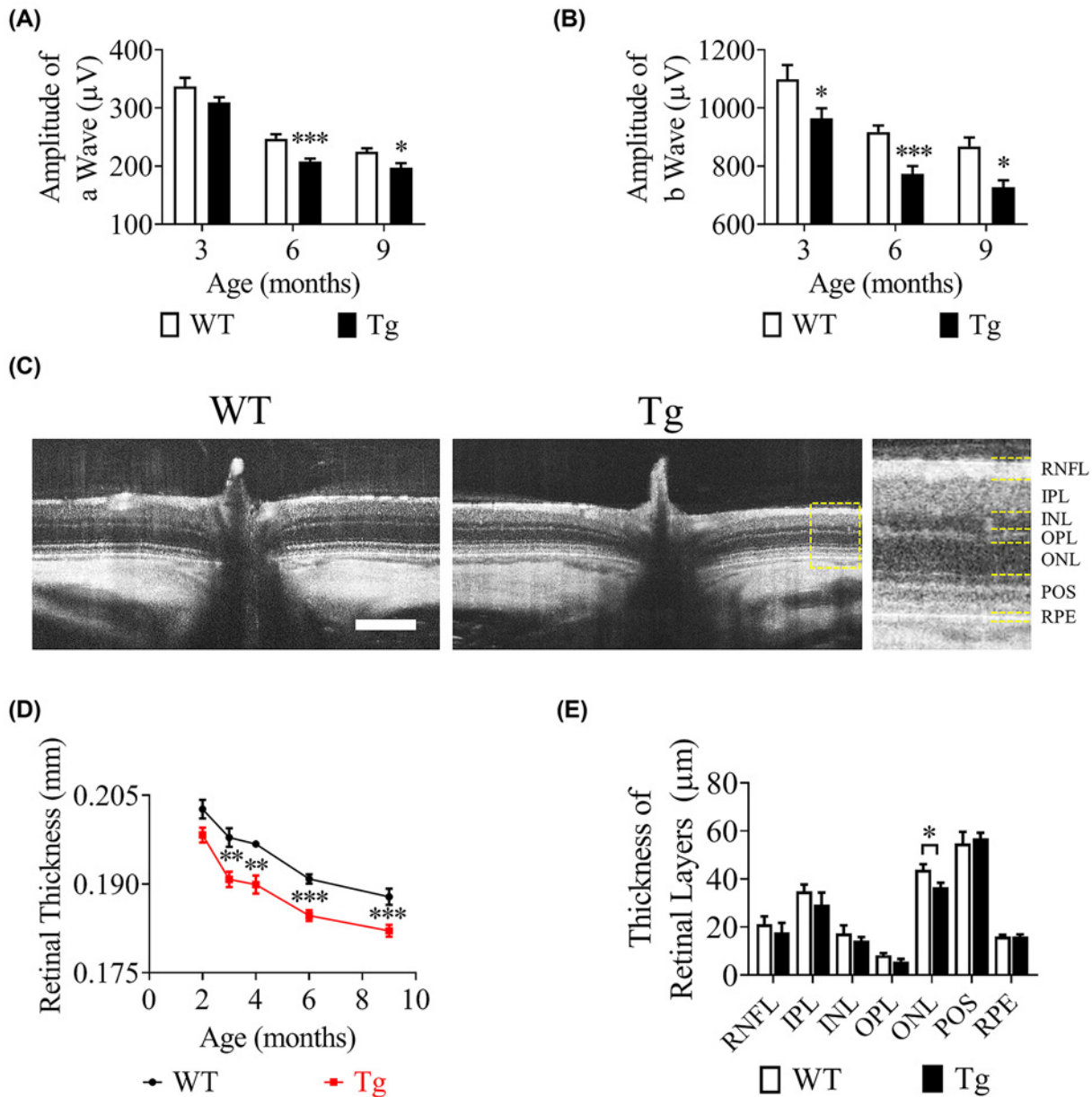
Figure 1. Retinal dysfunction and degeneration in hCRP-Tg rats

(**A**,**B**) Scotopic ERG a-wave (A) and b-wave (B) were measured in age-matched WT rats and hCRP-Tg rats (Tg) at indicated ages. Light intensity of 600 cd.s/m^2 was used. (**C**) Representative images of OCT of the retina in 6-month-old WT and hCRP-Tg rats. Scale bar = 200 μm. (**D**) Quantification of total retinal thickness measured by OCT in WT rats and hCRP-Tg rats. (**E**) Quantification of individual retinal layers including the retinal nerve fiber layer (RNFL), inner plexiform layer (IPL), inner nuclear layer (INL), outer plexiform layer (OPL), outer nuclear layer (ONL), photoreceptor outer segments (POS), and retinal pigment epithelium (RPE) in 6-month-old WT and hCRP-Tg rats. Data were presented as mean $\pm$ SEM ($n=8$–12). *$P<0.05$, **$P<0.01$, ***$P<0.001$.

the maximal responses of ERG, maximum light flash stimulation (600 cd.s/m^2) was selected for comparison. At the age of 3 months, hCRP-Tg rats did not display any significant reduction in amplitudes of scotopic a-wave compared with WT rats (Figure 1A). At the age of 6 and 9 months, hCRP-Tg rats displayed significantly reduced amplitudes of scotopic a-wave compared with WT rats (Figure 1A). At all age points, there was a significant decrease in scotopic b-wave amplitudes in hCRP-Tg rats compared with those in age-matched WT rats (Figure 1B).
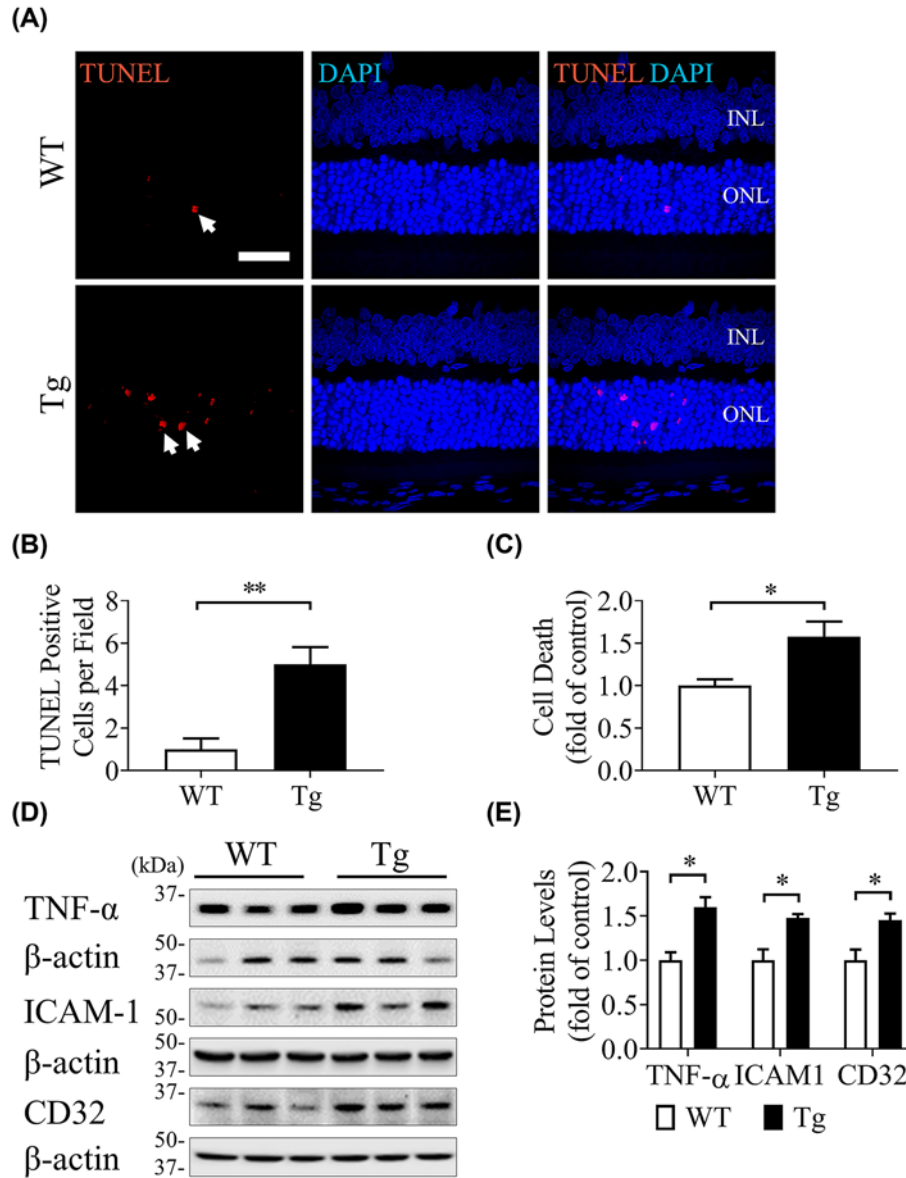
Figure 2. Up-regulated retinal inflammation and activation of CD32/NF-κB signaling in the retina of hCRP-Tg rats
(**A**) Representative images of TUNEL staining in retinal sections of 6-month-old WT rats and hCRP-Tg rats (Tg). White arrows indicate TUNEL-positive cells (red). Scale bar = 25 μm. (**B**) Quantification of TUNEL-positive cells. (**C**) Cell death ELISA was performed in the retina of WT rats and hCRP-Tg rats at the age of 6 months. (**D**) Representative images of Western blotting for TNF-α, ICAM-1, and CD32 in the retinas of 6 month-old WT rats and hCRP-Tg rats. Each lane represented a single rat. (**E**) Densitometry quantification of TNF-α, ICAM-1, and CD32 in (D). Data were presented as mean ± SEM (n=8–12). *P<0.05, **P<0.01. Abbreviation: INL, inner nuclear layer.

Retinal degeneration in hCRP-Tg rats

As measured by OCT, hCRP-Tg rats showed significant decreases in total retinal thickness at 3, 4, 6, and 9 months of age compared with age-matched WT rats (Figure 1C,D). The thickness of individual retinal layers was analyzed in 6-month-old rats. There was a significant decrease in the outer nuclear layer (ONL) thickness in hCRP-Tg rats compared with WT rats (Figure 1E). To test whether hCRP leads to retinal degeneration by inducing retinal apoptotic death, TUNEL staining and cell death ELISA were performed. There were increased TUNEL-positive cells primarily in the ONL of the retinas of hCRP-Tg rats compared with those in WT rats (Figure 2A). hCRP-Tg showed a four-fold

increase in TUNEL-positive cells over that in WT controls (Figure 2B). Consistently, cell death ELISA showed increased apoptosis in the retinas of hCRP-Tg rats (Figure 2C).

In fundus images, hCRP-Tg rats showed a similar density and branch of retinal blood vessels compared with their age-matched WT controls (Supplementary Figure S3A). There was no significant difference between WT rats and hCRP-Tg rats in retinal vascular permeability as shown by the permeability assay using Evans Blue as a tracer (Supplementary Figure S3B). Furthermore, albumin levels in the perfused retinas of hCRP-Tg were similar to those in WT rats (Supplementary Figure S3C,D). Finally, hCRP-Tg rats demonstrated similar numbers of adherent leukocytes per flat-mounted retina compared with those in the controls as shown by leukostasis assay (Supplementary Figure S3E,F). Thus, elevated hCRP levels resulted in retinal neurodegeneration while not affecting retinal vasculature in non-diabetic conditions.

hCRP-induced retinal inflammation and oxidative stress were associated with the up-regulation of the hCRP receptor CD32

As oxidative stress and inflammation in the retina are known to play key pathogenic roles in DR, we measured immunostained 3-NT and pro-inflammatory markers in the retina of hCRP-Tg rats. Immunostaining results showed that there was an increase in 3-NT signal in the retinal section of 6-month-old hCRP-Tg rats compared with those in age-matched WT rats, suggesting that hCRP induces oxidative stress in the retina (Supplementary Figure S4A,B). As shown by Western blot analysis, there were increased levels of pro-inflammatory factor (TNF-α) and cell adhesion molecule (ICAM-1) in the retinas of 6-month-old hCRP-Tg rats compared with those in age-matched WT rats (Figure 2D,E). As hCRP is known to bind to its receptors, CD32 and CD64, to confer its pro-inflammatory effect [20], we measured CD32 and CD64 in the retina. As shown by Western blot analysis, both of CD32 and CD64 were expressed in the retinas (Figure 2D and Supplementary Figure S5A). CD32 was significantly up-regulated (Figure 2D,E), while CD64 levels showed no significant changes in the retinas of 6-month-old hCRP-Tg rats relative to those in WT rats (Supplementary Figure S5A,C), suggesting that hCRP induced overexpression of CD32 and, subsequently, oxidative stress and inflammation in the retina.

hCRP induced cell death and oxidative stress in cultured retinal cells

We further investigated the role of hCRP in cell death and oxidative stress in cultured retinal cells. As measured by cell death ELISA, purified hCRP increased apoptosis events by approximately two-fold in 661W and rMC-1 cells (Figure 3A). As measured by Trypan Blue exclusion assay, purified hCRP significantly decreased the viability of these cells compared with the untreated group or BSA-treated group (Figure 3B). In addition, as shown by the DCF method, hCRP also increased the production of ROS by approximately four-fold in 661W and rMC-1 cells (Figure 3C), consistent with the result of 3-NT staining in the retina of hCRP-Tg rats. These results in cultured cells suggest that the effects of hCRP on oxidative stress are through direct interactions with retinal cells.

Elevated hCRP levels promoted the retinal dysfunction and cell death in diabetes

To evaluate the impact of high levels of hCRP on retinal function under diabetic conditions, diabetes was induced in WT rats and hCRP-Tg rats at the age of 2 months. To rule out the potential impact of diabetes on the expression of hCRP, hCRP levels in retinas were measured by Western blot analysis in non-diabetic hCRP-Tg rats and diabetic hCRP-Tg rats. There was no significant difference of hCRP levels in STZ-induced diabetic hCRP-Tg rats relative to those in non-diabetic hCRP-Tg rats (Supplementary Figure S5A,B). Scotopic ERG was recorded at 1, 4, and 7 months after the onset of diabetes. At 1 month after the onset of diabetes, diabetic hCRP-Tg rats showed no significant decline in the scotopic a-wave and b-wave compared with diabetic WT rats (Figure 4A,B). However, significant declines of scotopic a-wave and b-wave were observed in diabetic hCRP-Tg rats compared with diabetic WT rats at 4 and 7 months of diabetes (Figure 4A,B). Moreover, the implicit time of scotopic a-wave and b-wave was recorded and analyzed in 6-month-old rats. There was no significant increase in implicit time of scotopic a-wave and b-wave in non-diabetic or diabetic hCRP-Tg rats compared with those in WT rats (Supplementary Figure S2C,D). To determine if progressive declines of retinal function were associated with increased retinal cell death in diabetic hCRP-Tg rats, we measured apoptosis in the retina. As measured by TUNEL, there was an increase in TUNEL-positive cells in the retina in diabetic hCRP-Tg rats compared with those in diabetic WT rats (Figure 4C). The retinas of diabetic hCRP-Tg rats showed approximately two-fold increase in TUNEL-positive cells over those in diabetic WT rats (Figure 4D). Similarly, cell death ELISA demonstrated that retinal apoptotic cells were increased by approximately 1.5-fold in diabetic hCRP-Tg rats compared with diabetic WT rats (Figure 4E). To identify the cell types that were affected
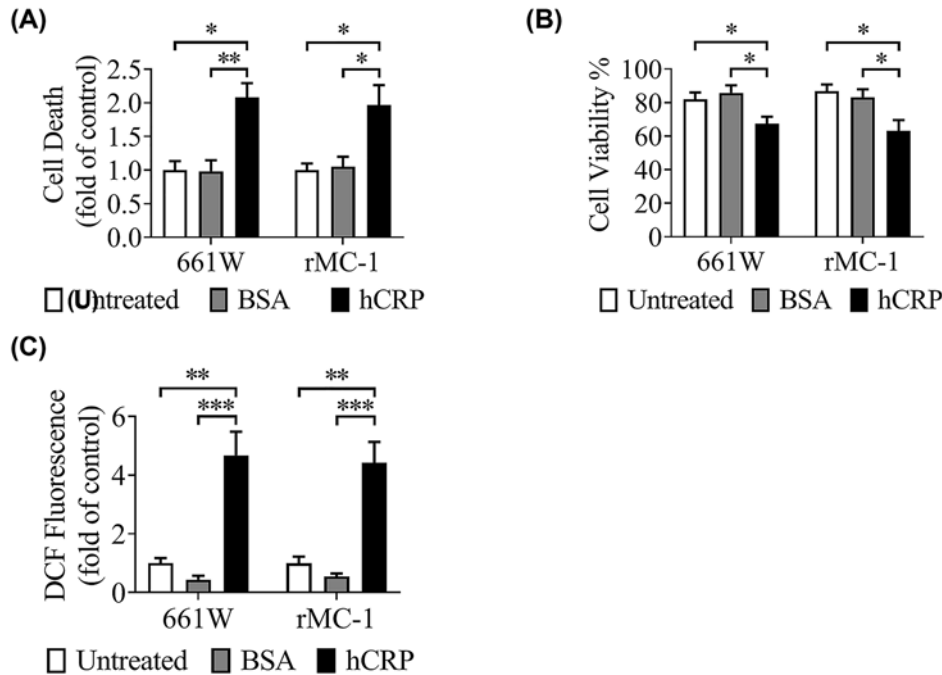
Figure 3. Higher rate of apoptosis and oxidative stress in hCRP-treated cells
(**A**) Cell death ELISA was performed in 661W and rMC-1 cells treated with hCRP (10 μg/ml, 24 h). Untreated group and BSA-treated group were used as control. (**B**) Viable cells were counted with Trypan Blue staining in untreated, BSA-treated, and hCRP (10 μg/ml, 24 h)-treated 661W and rMC-1 cells. (**C**) The oxidative stress was measured in hCRP (10 μg/ml, 3 h)-treated 661W and rMC-1 cells and the controls. After hCRP treatment, cells were incubated with CM-H$_2$DCFDA (1:5000 dilution) for 0.5 h, and the DCF fluorescence signal was detected. Data were presented as mean ± SEM (n=6). *$P<0.05$, **$P<0.01$, ***$P<0.001$.

in retinal degeneration, the densities of retinal photoreceptor cells were quantified. Rhodopsin and PNA were used as markers for labeling rod outer segments and cone photoreceptors, respectively [40,41]. There was a significant decrease in the intensity of rhodopsin staining in diabetic hCRP-Tg rats relative to diabetic WT rats (Supplementary Figure S7A,B). There was a significant decrease in the density of PNA-positive cells in diabetic hCRP-Tg rats vs. diabetic WT rats (Supplementary Figure S8A,B). These results indicated that hCRP promoted retinal photoreceptor degeneration.

hCRP-induced retinal inflammation in diabetes was associated with the up-regulation of NF-κB signaling

To study whether hCRP can induce inflammation in the retina in diabetic condition, we measured the expression of inflammatory factors. Western blot analysis demonstrated a significant up-regulation of TNF-α and ICAM-1 levels in the retinas of diabetic hCRP-Tg rats compared with those of diabetic WT rats (Figure 5A–D). To address the mechanism underlying the pro-oxidative stress and pro-inflammatory effects of hCRP in diabetes, the activation of the NF-κB pathway was measured. As shown by Western blot analysis, there was a significant increase in phosphorylated IKKα (Ser^{180}) and IKKβ (Ser^{176}), as well as elevated levels of phosphorylated NF-κB p65 (Ser^{536}) in the retinas of diabetic hCRP-Tg rats compared with those in diabetic WT rats (Figure 5E–G and Supplementary Figure S5A,D). There were similar levels of total IKKα, IKKβ, and total NF-κB p65 between these two groups (Figure 5G). Meanwhile, to test the hypothesis whether Wnt signaling was regulated by hCRP, the activation of Wnt signaling was measured. As shown by Western blot analysis, there was no significant increase in total β-catenin in the retinas of hCRP-Tg rats compared with those in WT rats in non-diabetic condition or in diabetic conditions (Supplementary Figure S5E,F), suggesting that the pro-inflammatory effect of hCRP was not mediated through Wnt signaling. This finding was consistent with luciferase-based promoter activity assay *in vitro*. hCRP-treated rMC-1 cells or ARPE-19 cells did not show increased transcriptional activities of β-catenin compared with those in untreated group (Supplementary Figure S5G,H). Furthermore, hCRP did not promote Wnt3A ligand-induced Wnt signaling (Supplementary
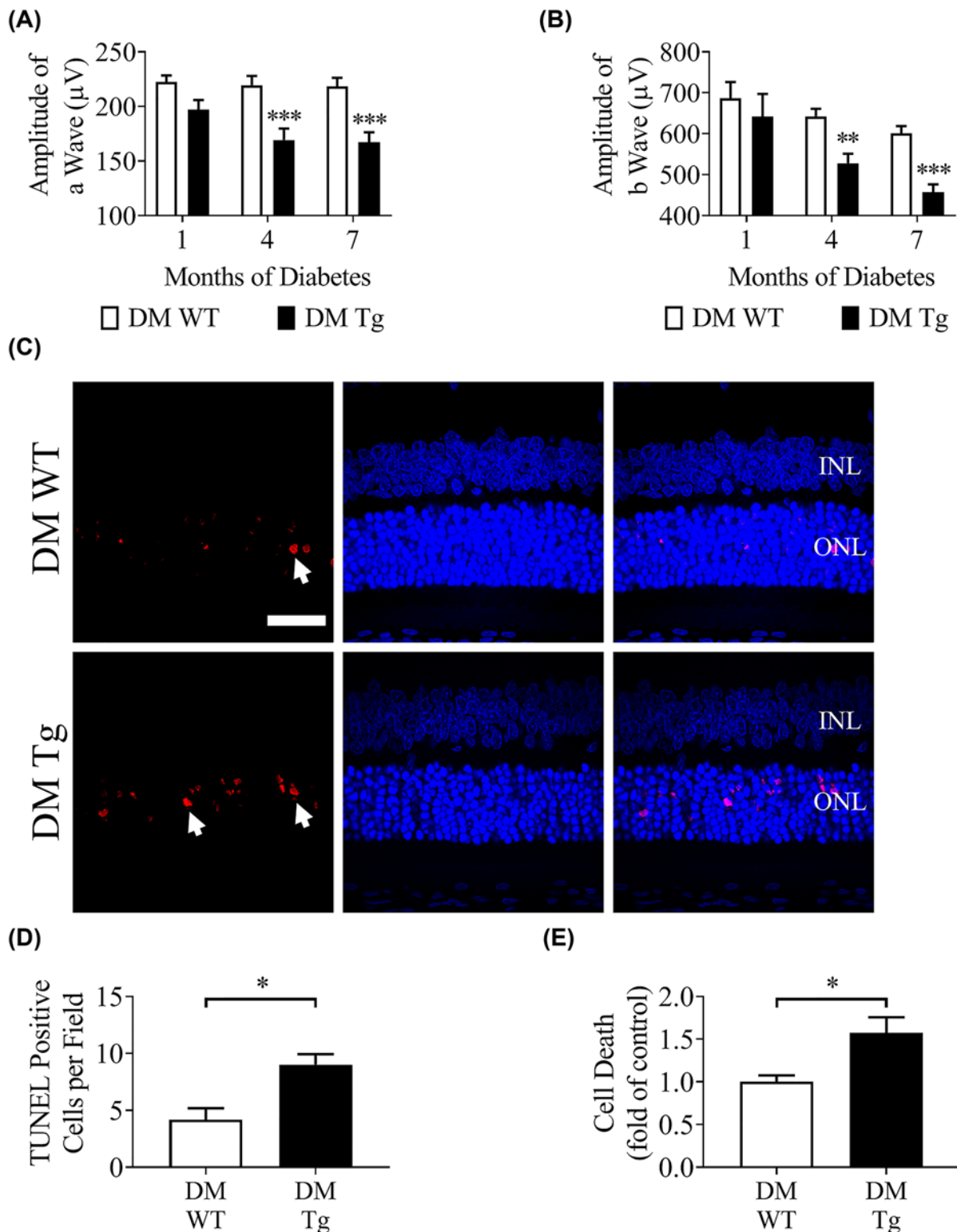
Figure 4. ERG decline and retinal cell death in STZ-induced diabetic hCRP-Tg rats

(**A**,**B**) Scotopic ERG a-wave (A) and b-wave (B) were measured in WT rats and hCRP-Tg rats (Tg) with indicated duration of STZ-induced diabetes (DM). Light intensity of 600 cd.s/m² was used. (**C**) Representative TUNEL images in retinal sections of 6-month-old diabetic WT rats and diabetic hCRP-Tg rats. White arrows indicate TUNEL-positive cells (red). Scale bar = 25 µm. (**D**) Quantification of TUNEL-positive cells (*n*=8–12). (**E**) Cell death ELISA was performed in the retinas of 6-month-old diabetic WT rats and diabetic hCRP-Tg rats (*n*=8–12). Data were presented as mean ± SEM. *P<0.05, **P<0.01, ***P<0.001. Abbreviation: INL, inner nuclear layer.
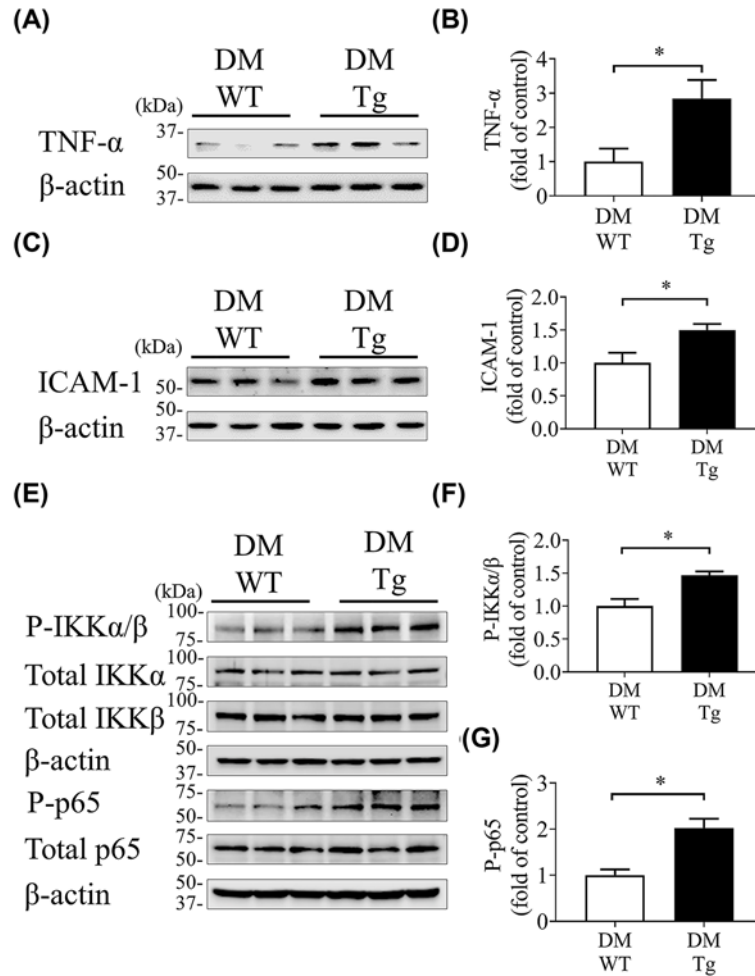
Figure 5. Increased retinal inflammation in diabetic hCRP-Tg rats

Retina homogenate from 6-month-old diabetic WT rats and diabetic hCRP-Tg rats were used for Western blot analysis. (**A**) Representative images of Western blotting for TNF-α. (**B**) Protein levels of TNF-α in A were quantified by densitometry. (**C**) Representative images of Western blotting for ICAM-1. (**D**) Protein levels of ICAM-1 in (C) were quantified by densitometry. (**E**) Representative images of Western blotting for phosphorylated IKKα/β (P-IKKα/β), total IKKα, total IKKβ, phosphorylated p65 (P-p65), and total p65 in the retinas. (**F**,**G**) Levels of P-IKKα/β and P-p65 were quantified and normalized to total IKKα and total p65, respectively. Data were presented as mean $\pm$ SEM (n=8–12). *P<0.05.

Figure S5G,H). Overall, these results suggested that hCRP-induced oxidative stress and inflammation likely through the NF-κB signaling, rather than the Wnt pathway.

To investigate if retinal vasculature was affected by inflammation, retinal leukostasis and acellular capillary formation were analyzed in 6-month-old diabetic WT rats and diabetic hCRP-Tg rats. We found that there was a significant increase in leukocytes adherent to the retinal vessels in diabetic hCRP-Tg rats compared with those in diabetic WT rats (Figure 6A,B). There was a significant increase in acellular capillaries in diabetic hCRP-Tg rats vs. WT rats (Figure 6C,D). To see if the CRP receptor was expressed in retinal vessels, the CD32 staining was performed in retinal sections of diabetic hCRP-Tg rats. We found that intense CD32 signals in the retinal vasculature as well as in the layer of photoreceptor outer segments (Supplementary Figure S6A). These results indicated that hCRP may promote retinal vascular cell death via CD32 in diabetes.

hCRP promoted the retinal NV and inflammation in the OIR model

As OIR is a well-accepted model of ischemia-induced retinal NV, we further investigated the role of hCRP in retinal NV using the OIR model. Under normoxic conditions, retinal vasculature reached the edge of the retina in both WT control rats and hCRP rats at P14, with no significant difference in the morphology, density, and distribution of retinal
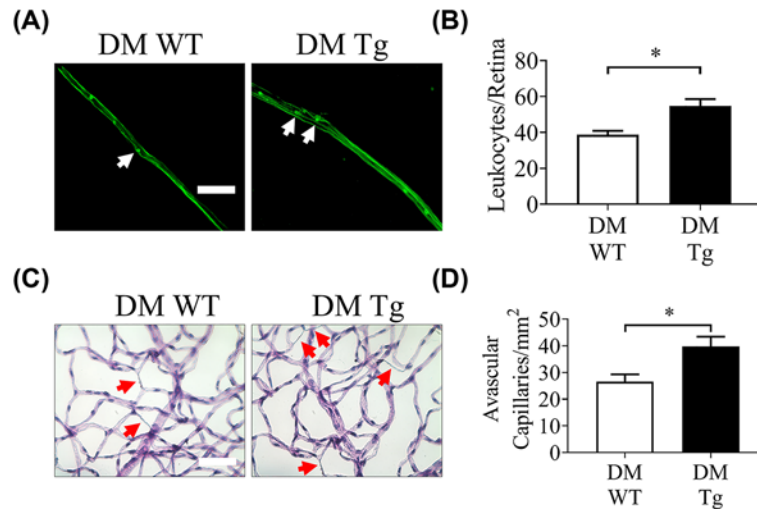
Figure 6. Increased retinal dysfunction in diabetic hCRP-Tg rats

(**A**) Representative images of leukostasis assay in 6-month-old WT rats and hCRP-Tg rats (Tg) with 4 months of STZ-induced diabetes (DM). White arrows indicate adherent leukocytes (green). Scale bar = 10 μm. (**B**) Adherent leukocytes were quantified in flat-mounted retinas of diabetic WT rats and hCRP-Tg rats. (**C**) Representative images showing trypsin disgested retinal vasculature from 6-month-old WT rats and hCRP-Tg rats. Red arrows indicate acellular capillaries. Scale bar = 50 μm. (**D**) Quantification data of acellular capillaries (AC) in C (*n*=4–5). Data were presented as mean ± SEM (*n*=8–12). *P<0.05.
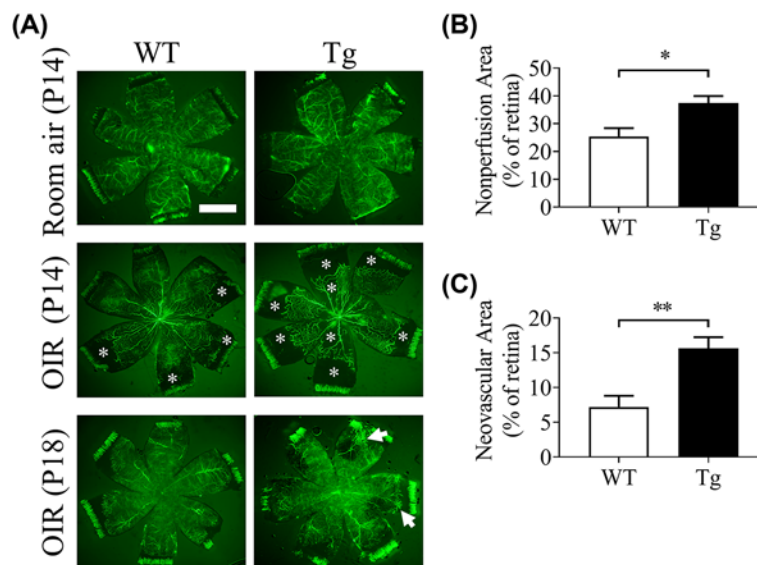

Figure 7. More severe retinal NV in hCRP-Tg rats with OIR

(**A**) Representative images of flat-mounted retinas from WT rats and hCRP-Tg rats with OIR or constant room air at postnatal days 14 (P14) and 18 (P18). White stars indicate non-perfusion areas. White arrows indicate neovascular area. Scale bar = 300 μm. (**B**) The percentage of the non-perfusion area in the flat-mounted retinas in WT rats and hCRP-Tg rats with OIR at P14. (**C**) The percentage of the neovascular area in the flat-mounted retina in WT rats and hCRP-Tg rats with OIR at P18. Data were presented as mean ± SEM (*n*=6). *P<0.05, **P<0.01.

vasculature between genotypes at P14 (Figure 7A). In contrast, the hCRP-Tg OIR rats showed enlarged non-perfusion areas in the retina relative to WT rats with OIR, indicating that hCRP may enhance the retinal vaso-obliteration induced by hyperoxia (Figure 7B). At P18, hCRP-Tg rats with OIR demonstrated an approximate 2.5-fold increase in the NV area compared with that in WT OIR rats (Figure 7C). Meanwhile, Western blotting demonstrated that VEGF
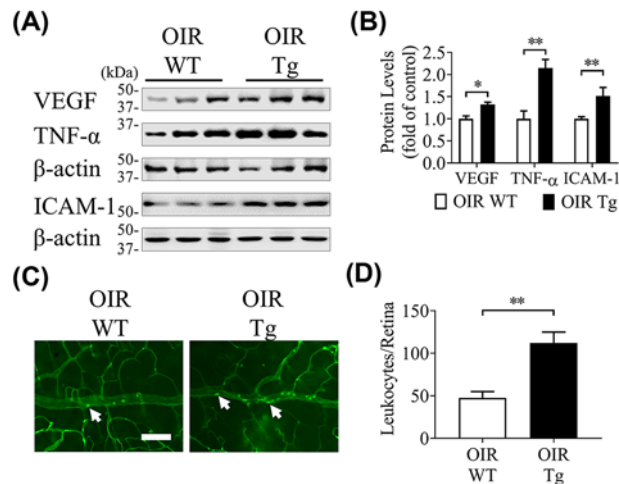
1623

Figure 8. Exacerbated retinal inflammation in hCRP-Tg rats with OIR

(**A**) Representative images of Western blotting for VEGF, TNF-α, and ICAM-1 in the retinas of WT rats and hCRP-Tg rats with OIR at P14. (**B**) Levels of VEGF, TNF-α, and ICAM-1 in (A) were quantified by densitometry. (**C**) Representative images of leukostasis assay in the retinas of WT pups and hCRP-Tg pups with OIR at P14. White arrows indicate adherent leukocytes. Scale bar = 20 μm. (**D**) Adherent leukocytes were quantified in flat-mounted retinas of WT pups and hCRP-Tg pups with OIR. Data were presented as mean $\pm$ SEM (n=8). *P<0.05, **P<0.01.

was significantly overexpressed in the retina of hCRP-Tg rats compared with WT rats, suggesting a pro-angiogenic effect of hCRP in the context of OIR (Figure 8A,B).

The retinal inflammation was measured in the OIR model. Pro-inflammatory factors, including TNF-α and ICAM-1, were up-regulated in the retinas of hCRP-Tg rats compared with those in WT rats in the OIR model (Figure 8A,B). Interestingly, different from the normoxic condition, OIR hCRP-Tg rats showed an approximate two-fold increase in leukocytes adherent to retinal vessels compared with WT rats with OIR (Figure 8C,D). Overall, these results suggested that high hCRP levels exacerbated retinal NV as well as inflammation in the context of OIR.

Discussion

CRP is a well-accepted biomarker of acute inflammation and is also associated with chronic low-grade inflammation and neurodegenerative diseases [42]. Prospective clinical studies have demonstrated a positive correlation between elevated CRP levels and Type 1 and Type 2 diabetes, as well as increased risks for diabetic complications, such as DR [9–11]. However, the pathogenic role of CRP in DR has never been investigated. The present study provides the evidence that elevated hCRP levels resulted in retinal dysfunction by causing retinal neural degeneration under non-diabetic conditions. Under diabetes conditions, elevated hCRP levels exacerbated retinal dysfunction, neural degeneration, inflammation, and vascular dysfunction. hCRP also exacerbated ischemia-induced retinal NV in the OIR model. Concerning the mechanism for the role of CRP in DR pathogenesis, we found that hCRP induced over-production of ROS and overexpression of pro-inflammatory factors under non-diabetic conditions, diabetic conditions, and in the OIR model, likely through CD32/NF-κB signaling, which is responsible at least partially for hCRP-induced retinal cell apoptosis and consequent retinal dysfunction. Taken together, our study has revealed that the elevated hCRP level in diabetes is a novel pathogenic mechanism and a potential therapeutic target for DR.

The normal range of serum CRP in healthy adults varies from 0.8 to 3.0 mg/l as measured by well-accepted high-sensitivity immunoassay [43]. Laursen et al. reported that 90th percentile of serum CRP was 21.4 mg/l in type 1 diabetic patients with retinopathy [44]. Our transgenic rat model showed that mean serum hCRP levels were from 28.5 mg/l in hCRP-Tg rats aged at 3 months, suggesting that levels of hCRP in this model are physiologically relevant to diabetic patients. Moreover, STZ-induced diabetes did not change the retinal levels of hCRP in hCRP-Tg rats, indicating that our transgenic rats are an appropriate model for specifically investigating the role of hCRP in diabetes. In addition, unlike hCRP, endogenous rat CRP (rCRP) is not an acute-phase protein, which is not able to activate complement [45–47]. Thus, we applied this transgenic model with hCRP overexpression.

DR was traditionally known as a retinal vascular complication [48]. However, later studies showed that retinal neuron degeneration also plays a role in the vision loss in patients with DR [5,49]. The present study demonstrated that

high levels of hCRP induced declines of ERG a-wave and b-wave, increased apoptosis in the retina, and decreased retinal thickness in non-diabetic condition, suggesting that overexpressed hCRP itself can cause retinal neurodegeneration. To further identify the direct effect of hCRP on retinal cells, we applied purified hCRP to cultured cell lines derived from retinal Müller cells and from photoreceptor cells. The results showed that hCRP induced apoptosis in these cultured retinal cells. These *in vivo* and *in vitro* results confirmed that hCRP directly acted on retinal cells and induced apoptotic cell death. Here, we showed for the first time that hCRP was implicated in pro-apoptotic effect in ocular disorders, which was consistent with previous findings in the cardiovascular system and immune system [14,20,50]. Ryu et al. described the apoptotic changes of vascular smooth muscle cells in response to hCRP [14]. In addition, Kim et al. reported that hCRP stimulated apoptosis by inducing G_2/M phase arrest in the cell cycle in monocytes [37].

To study the impact of elevated hCRP levels on retinal neurons and vasculature in diabetes, we induced diabetes in WT rats and hCRP-Tg rats. As demonstrated by TUNEL staining, most of apoptotic cells were located in the ONL, indicating hCRP accelerated death of retinal photoreceptors in diabetes. We confirmed this observation by quantifying the rod and cone photoreceptor cells. We found that hCRP promoted diabetes-induced loss of retinal photoreceptors. This observation can be explained by more intense expression of hCRP and CD32 in the layer of photoreceptor outer segments (POSs), which may mediate the direct detrimental effect in photoreceptor cells. Moreover, photoreceptors generate high levels of ROS and they are also highly vulnerable to oxidative stress [2]. hCRP in the local microenvironment may worsen the photoreceptor apoptosis induced by oxidative stress under diabetic conditions. Meanwhile, we also observed that hCRP worsened the retinal vascular inflammation and vascular cell death in diabetes. We found that hCRP overexpression resulted in more leukocytes attached to retinal vasculature and more acellular capillaries in the retina in diabetes. Given that high hCRP level in the circulation and intense expression of CRP receptor, CD32, in retinal vasculature, hCRP may accelerate diabetes-induced retinal vascular damage via CD32. These findings suggest that elevated hCRP levels in diabetes exacerbate diabetes-induced retinal inflammation, neuronal degeneration, and vascular damage.

The OIR model, one of the well-accepted models for ischemia-induced retinal NV, was used to investigate the pathogenic role of hCRP in retinal NV. In the OIR model, high levels of hCRP exacerbated ischemia-induced retinal NV. Interestingly, elevated hCRP can enlarge the non-perfusion area in the retinas of pups exposed to hyperoxic conditions, as well as promote the later pathological vessel formation in a relative hypoxic environment. This may, presumably, result from more severe vaso-obliteration in hCRP-Tg pups likely via more severe leukostasis. Consistently, we observed enhanced ischemia-induced VEGF overexpression in the retinas of hCRP-Tg pups with OIR. This pro-angiogenic effect of hCRP was consistent with a previous study, which reported that there was an increased VEGF level in the conditioned medium of CRP-treated adipose-derived stem cells, resulting in increased tube formation in human umbilical vein endothelial cells (HUVECs) [51]. However, some authors have observed that hCRP inhibited VEGF production and angiogenesis in non-ocular tissues [52,53]. The disparity regarding the role of hCRP in angiogenesis suggests that CRP may play distinct roles under different conditions.

There are three potential mechanisms for the pathogenic role of hCRP in DR. First, we found that elevated hCRP levels up-regulated the expression of pro-inflammatory factors in both physiological and pathological conditions, including diabetic condition and hypoxic condition in the OIR model. However, hCRP-Tg rats showed a significant increase in retinal leukostasis only in pathological condition, suggesting that elevated hCRP may play a deleterious role in high glucose-induced or hypoxia-induced up-regulation of pro-inflammatory cytokines in the retinas. Second, hCRP may promote diabetes-induced oxidative stress. Immunostaining of 3-NT demonstrated enhanced 3-NT signals in retinal sections of diabetic hCRP-Tg rats compared with diabetic WT rats, supporting that hCRP led to more severe oxidative stress in the retinas. Third, hCRP may contribute to DR by enhancing retinal NV. As we know, hyperglycemia and metabolic disorders in diabetes result in alterations of retinal vasculature, leading to relative hypoxic condition in the retina [54]. Among various angiogenic factors, VEGF plays a key role in the ischemia-induced NV in DR. We found that overexpression of hCRP can up-regulate the VEGF level in the retina of OIR model. The elevated VEGF level in hCRP-Tg of OIR model may occur indirectly as a result of increased vaso-obliteration. Taken together, these results suggest that the hCRP-induced inflammation, oxidative stress, and angiogenesis may contribute to the impairment of the retinal neurovascular unit under diabetic conditions.

To investigate the signaling pathway underlying hCRP-induced pathological change, we first measured retinal levels of the hCRP receptor, CD32. Previous studies have identified CD32 as the major CRP receptor in various tissues. Du Clos et al. identified CD32 as a major CRP receptor in monocytes and neutrophils based on the interaction between CRP and CD32 transfected cells with flow cytometry [20,55]. Moreover, CD32 was shown to be one of the CRP receptors in human aortic endothelial cells (HAECs) and kidney tubular epithelial cells using a neutralizing antibody to CD32 [18,56]. In addition, CRP-treated endothelial cells and the kidney of hCRP-Tg mice showed up-regulation

of CD32 [18,56]. Our results first demonstrated that overexpressed hCRP was associated with the up-regulation of CD32 in the retina. This is consistent with the findings in the non-ocular tissues. Second, since the NF-κB pathway was downstream of CD32, and aberrant activation of the NF-κB pathway resulted in the up-regulation of pro-inflammatory factors, we tested whether hCRP-induced DR pathogenesis was associated with the up-regulation of this signaling pathway [57,58]. Our results demonstrated that overexpression of hCRP resulted in the activation of the NF-κB pathway, which may further enhance inflammation, ROS generation, and NV. These pathological alterations may contribute to the apoptotic cell death in the retina, resulting in retinal degeneration and impaired visual function. This notion was supported by observations reported in previous studies [18,57,59,60]. Moreover, since Wnt pathway was also a well-accepted pro-inflammatory signaling in DR [61], we also studied the cross-talk between hCRP and Wnt signaling. However, we found that hCRP did not enhance Wnt pathway activation based on both luciferase-base β-catenin transcriptional activity assay or Western blot analysis for β-catenin levels, suggesting that hCRP effect is unlikely mediated by Wnt signaling. Taken together, these results indicated that hCRP drove the inflammation and NV, at least partially, through NF-κB signaling.

Our study has several limitations. First, we only tested the hCRP role in DR pathogenesis in a type 1 diabetic model. The question of whether hCRP plays a pathogenic role in DR of type 2 diabetes warrants further investigation. Second, increased circulation levels of hCRP may induce systemic inflammatory effect, which may result in secondary pathological changes in ocular tissues. Third, hCRP may drive the inflammation through multiple signaling pathways. We cannot rule out potential signaling pathways in addition to NF-κB signaling.

In summary, our study showed for the first time that hCRP is not only a biomarker, but also a pathogenic factor in DR. hCRP impaired the retinal neurovascular unit at least partly by promoting inflammation, ROS generation, and NV in the retinas. The present study suggests that the up-regulated hCRP-CD32-NF-κB pathway may represent a new pathogenic mechanism for DR and that hCRP could be a potential therapeutic target for DR.

Clinical perspectives

- **Background:** Elevated blood levels of hCRP are associated with DR. However, the pathogenic role of hCRP in DR has not been fully investigated.

- **Summary of results:** Overexpression of hCRP resulted in the up-regulation of NF-κB signaling, contributing to the retinal dysfunction and degeneration in diabetes. Moreover, elevated hCRP levels promoted the retinal NV and inflammation in the model of OIR.

- **Significance:** The present study suggests that the up-regulated hCRP-CD32-NF-κB pathway may represent a new pathogenic mechanism for DR and that hCRP could be a potential therapeutic target for DR.

Competing Interests

The authors declare that there are no competing interests associated with the manuscript.

Funding

Author Contribution

F.Q. and X.M. performed experiments, acquired and analyzed data, and wrote the manuscript. J.C., Q.C., W.W., W.L., and K.Z. conducted experiments and acquired data. Y.-H.S. and Y.W. performed the literature search, wrote the manuscript. J.-x.M. and Q. S. designed the research, analyzed data, wrote and edited the manuscript. J.-X.M. is the guarantor of this work and, as such, had full access to all the data in the present study and takes responsibility for the integrity of the data and the accuracy of the data analysis.

PORTLAND PRESS

Acknowledgements

Abbreviations

CRP, C-reactive protein; DCF, Dichlorodihydrofluorescein; DMEM, Dulbecco's Modified Eagle's Medium; DR, Diabetic retinopathy; ERG, Electroretinography; FBS, Fetal bovine serum; hCRP-Tg, Human CRP transgenic; ICAM-1, Intercellular adhesion molecule-1; IKK, Inhibitor of nuclear factor kappa-B kinase; NPDR, Non-proliferative DR; NV, Neovascularization; OCT, Optical coherence tomography; OIR, Oxygen-induced retinopathy; ONL, Outer nuclear layer; PDR, Proliferative DR; PNA, Peanut agglutinin; rMC-1, Rat retinal Müller cell; ROS, Reactive oxygen species; STZ, Streptozotocin; TCF, T cell factor; TNF-α, Tumor necrosis factor-α; TUNEL, Terminal deoxynucleotidyl transferase dUTP nick end labeling; VEGF, Vascular endothelial growth factor; WT, Wild-type; 3-NT, 3-Nitrotyrosine.

References

1 Cheung, N., Mitchell, P. and Wong, T.Y. (2010) Diabetic retinopathy. *Lancet* **376**, 124–136, https://doi.org/10.1016/S0140-6736(09)62124-3

2 Duh, E.J., Sun, J.K. and Stitt, A.W. (2017) Diabetic retinopathy: current understanding, mechanisms, and treatment strategies. *JCI Insight* **2**, 1–13, https://doi.org/10.1172/jci.insight.93751

3 Wang, J., Xu, X., Elliott, M.H., Zhu, M. and Le, Y.Z. (2010) Muller cell-derived VEGF is essential for diabetes-induced retinal inflammation and vascular leakage. *Diabetes* **59**, 2297–2305, https://doi.org/10.2337/db09-1420

4 Stitt, A.W., Curtis, T.M., Chen, M., Medina, R.J., McKay, G.J., Jenkins, A. et al. (2016) The progress in understanding and treatment of diabetic retinopathy. *Prog. Retin. Eye Res.* **51**, 156–186, https://doi.org/10.1016/j.preteyeres.2015.08.001

5 Antonetti, D.A., Klein, R. and Gardner, T.W. (2012) Diabetic retinopathy. *N. Engl. J. Med.* **366**, 1227–1239, https://doi.org/10.1056/NEJMra1005073

6 Kowluru, R.A. and Mishra, M. (2015) Oxidative stress, mitochondrial damage and diabetic retinopathy. *Biochim. Biophys. Acta* **1852**, 2474–2483, https://doi.org/10.1016/j.bbadis.2015.08.001

7 Calderon, G.D., Juarez, O.H., Hernandez, G.E., Punzo, S.M. and De la Cruz, Z.D. (2017) Oxidative stress and diabetic retinopathy: development and treatment. *Eye* **31**, 1122–1130, https://doi.org/10.1038/eye.2017.64

8 Molins, B., Romero-Vazquez, S., Fuentes-Prior, P., Adan, A. and Dick, A.D. (2018) C-reactive protein as a therapeutic target in age-related macular degeneration. *Front. Immunol.* **9**, 808, https://doi.org/10.3389/fimmu.2018.00808

9 Freeman, D.J., Norrie, J., Caslake, M.J., Gaw, A., Ford, I., Lowe, G.D. et al. (2002) C-reactive protein is an independent predictor of risk for the development of diabetes in the West of Scotland Coronary Prevention Study. *Diabetes* **51**, 1596–1600, https://doi.org/10.2337/diabetes.51.5.1596

10 Chase, H.P., Cooper, S., Osberg, I., Stene, L.C., Barriga, K., Norris, J. et al. (2004) Elevated C-reactive protein levels in the development of type 1 diabetes. *Diabetes* **53**, 2569–2573, https://doi.org/10.2337/diabetes.53.10.2569

11 Rajab, H.A., Baker, N.L., Hunt, K.J., Klein, R., Cleary, P.A., Lachin, J. et al. (2015) The predictive role of markers of Inflammation and endothelial dysfunction on the course of diabetic retinopathy in type 1 diabetes. *J. Diabetes Complications* **29**, 108–114, https://doi.org/10.1016/j.jdiacomp.2014.08.004

12 Sasongko, M.B., Wong, T.Y., Jenkins, A.J., Nguyen, T.T., Shaw, J.E. and Wang, J.J. (2015) Circulating markers of inflammation and endothelial function, and their relationship to diabetic retinopathy. *Diabetic Med.* **32**, 686–691, https://doi.org/10.1111/dme.12640

13 Song, J., Chen, S., Liu, X., Duan, H., Kong, J. and Li, Z. (2015) Relationship between C-reactive protein level and diabetic retinopathy: a systematic review and meta-analysis. *PLoS ONE* **10**, e0144406, https://doi.org/10.1371/journal.pone.0144406

14 Ryu, J., Lee, C.W., Shin, J.A., Park, C.S., Kim, J.J., Park, S.J. et al. (2007) FcgammaRIIa mediates C-reactive protein-induced inflammatory responses of human vascular smooth muscle cells by activating NADPH oxidase 4. *Cardiovasc. Res.* **75**, 555–565, https://doi.org/10.1016/j.cardiores.2007.04.027

15 Fujii, H., Li, S.H., Szmitko, P.E., Fedak, P.W. and Verma, S. (2006) C-reactive protein alters antioxidant defenses and promotes apoptosis in endothelial progenitor cells. *Arterioscler. Thromb. Vasc. Biol.* **26**, 2476–2482, https://doi.org/10.1161/01.ATV.0000242794.65541.02

16 Kobayashi, S., Inoue, N., Ohashi, Y., Terashima, M., Matsui, K., Mori, T. et al. (2003) Interaction of oxidative stress and inflammatory response in coronary plaque instability: important role of C-reactive protein. *Arterioscler. Thromb. Vasc. Biol.* **23**, 1398–1404, https://doi.org/10.1161/01.ATV.0000081637.36475.BC

17 Zhong, Y., Cheng, C.F., Luo, Y.Z., Tian, C.W., Yang, H., Liu, B.R. et al. (2015) C-reactive protein stimulates RAGE expression in human coronary artery endothelial cells in vitro via ROS generation and ERK/NF-kappaB activation. *Acta Pharmacol. Sin.* **36**, 440–447, https://doi.org/10.1038/aps.2014.163

18 Liu, F., Chen, H.Y., Huang, X.R., Chung, A.C., Zhou, L., Fu, P. et al. (2011) C-reactive protein promotes diabetic kidney disease in a mouse model of type 1 diabetes. *Diabetologia* **54**, 2713–2723, https://doi.org/10.1007/s00125-011-2237-y

19 Badimon, L., Pena, E., Arderiu, G., Padro, T., Slevin, M., Vilahur, G. et al. (2018) C-reactive protein in atherothrombosis and angiogenesis. *Front. Immunol.* **9**, 430, https://doi.org/10.3389/fimmu.2018.00430

20 Sproston, N.R. and Ashworth, J.J. (2018) Role of C-reactive protein at sites of inflammation and infection. *Front. Immunol.* **9**, 754, https://doi.org/10.3389/fimmu.2018.00754

21 Li, Q., Ma, Y., Li, W., Xu, W., Ma, L., Fu, G. et al. (2014) A promoter that drives gene expression preferentially in male transgenic rats. *Transgenic Res.* **23**, 341–349, https://doi.org/10.1007/s11248-013-9773-9

22 Li, Q., Xu, W., Xue, X., Wang, Q., Han, L., Li, W. et al. (2016) Presence of multimeric isoforms of human C-reactive protein in tissues and blood. *Mol. Med. Rep.* **14**, 5461–5466, https://doi.org/10.3892/mmr.2016.5922

23 Qiu, F., Meng, T., Chen, Q., Zhou, K., Shao, Y., Matlock, G. et al. (2019) Fenofibrate-loaded biodegradable nanoparticles for the treatment of experimental diabetic retinopathy and neovascular age-related macular degeneration. *Mol. Pharm.* **16**, 1958–1970, https://doi.org/10.1021/acs.molpharmaceut.8b01319

24 Gammons, M.V. and Bates, D.O. (2016) Models of oxygen induced retinopathy in rodents. *Methods Mol. Biol.* **1430**, 317–332, https://doi.org/10.1007/978-1-4939-3628-1˙22

25 Chen, Q., Qiu, F., Zhou, K., Matlock, H.G., Takahashi, Y., Rajala, R.V.S. et al. (2017) Pathogenic role of microRNA-21 in diabetic retinopathy through downregulation of PPARalpha. *Diabetes* **66**, 1671–1682, https://doi.org/10.2337/db16-1246

26 Hu, Y., Chen, Y., Ding, L., He, X., Takahashi, Y., Gao, Y. et al. (2013) Pathogenic role of diabetes-induced PPAR-alpha down-regulation in microvascular dysfunction. *Proc. Natl. Acad. Sci. U.S.A.* **110**, 15401–15406, https://doi.org/10.1073/pnas.1307211110

27 Ding, L., Cheng, R., Hu, Y., Takahashi, Y., Jenkins, A.J., Keech, A.C. et al. (2014) Peroxisome proliferator-activated receptor α protects capillary pericytes in the retina. *Am. J. Pathol.* **184**, 2709–2720, https://doi.org/10.1016/j.ajpath.2014.06.021

28 Chen, Y., Hu, Y., Lin, M., Jenkins, A.J., Keech, A.C., Mott, R. et al. (2013) Therapeutic effects of PPARα agonists on diabetic retinopathy in type 1 diabetes models. *Diabetes* **62**, 261–272, https://doi.org/10.2337/db11-0413

29 Tomasek, J.J., Haaksma, C.J., Schwartz, R.J., Vuong, D.T., Zhang, S.X., Ash, J.D. et al. (2006) Deletion of smooth muscle alpha-actin alters blood-retina barrier permeability and retinal function. *Invest. Ophthalmol. Vis. Sci.* **47**, 2693–2700, https://doi.org/10.1167/iovs.05-1297

30 Chen, Q., Takahashi, Y., Oka, K. and Ma, J.X. (2016) Functional differences of very-low-density lipoprotein receptor splice variants in regulating Wnt signaling. *Mol. Cell. Biol.* **36**, 2645–2654, https://doi.org/10.1128/MCB.00235-16

31 Shin, Y., Moiseyev, G., Petrukhin, K., Cioffi, C.L., Muthuraman, P., Takahashi, Y. et al. (2018) A novel RPE65 inhibitor CU239 suppresses visual cycle and prevents retinal degeneration. *Biochim. Biophys. Acta Mol. Basis Dis.* **1864**, 2420–2429, https://doi.org/10.1016/j.bbadis.2018.04.014

32 Crowe, A.R. and Yue, W. (2019) Semi-quantitative determination of protein expression using immunohistochemistry staining and analysis: an integrated protocol. *Bioprotocol* **9**, 1–15, https://doi.org/10.21769/BioProtoc.3465

33 Zhang, B. and Ma, J.X. (2008) SERPINA3K prevents oxidative stress induced necrotic cell death by inhibiting calcium overload. *PLoS ONE* **3**, e4077, https://doi.org/10.1371/journal.pone.0004077

34 Tan, E., Ding, X.Q., Saadi, A., Agarwal, N., Naash, M.I. and Al-Ubaidi, M.R. (2004) Expression of cone-photoreceptor-specific antigens in a cell line derived from retinal tumors in transgenic mice. *Invest. Ophthalmol. Vis. Sci.* **45**, 764–768, https://doi.org/10.1167/iovs.03-1114

35 Cui, C.J., Li, S., Zhu, C.G., Sun, J., Du, Y., Zhang, Y. et al. (2016) Enhanced pro-protein convertase subtilisin/kexin type 9 expression by C-reactive protein through p38MAPK-HNF1α pathway in HepG2 cells. *J. Cell. Mol. Med.* **20**, 2374–2383, https://doi.org/10.1111/jcmm.12931

36 Chen, J., Gu, Z., Wu, M., Yang, Y., Zhang, J., Ou, J. et al. (2016) C-reactive protein can upregulate VEGF expression to promote ADSC-induced angiogenesis by activating HIF-1α via CD64/PI3k/Akt and MAPK/ERK signaling pathways. *Stem Cell Res. Ther.* **7**, 114

37 Kim, Y., Ryu, J., Ryu, M.S., Lim, S., Han, K.O., Lim, I.K. et al. (2014) C-reactive protein induces G2/M phase cell cycle arrest and apoptosis in monocytes through the upregulation of B-cell translocation gene 2 expression. *FEBS Lett.* **588**, 625–631, https://doi.org/10.1016/j.febslet.2014.01.008

38 He, X., Cheng, R., Park, K., Benyajati, S., Moiseyev, G., Sun, C. et al. (2017) Pigment epithelium-derived factor, a noninhibitory serine protease inhibitor, is renoprotective by inhibiting the Wnt pathway. *Kidney Int.* **91**, 642–657, https://doi.org/10.1016/j.kint.2016.09.036

39 Lee, K., Hu, Y., Ding, L., Chen, Y., Takahashi, Y., Mott, R. et al. (2012) Therapeutic potential of a monoclonal antibody blocking the Wnt pathway in diabetic retinopathy. *Diabetes* **61**, 2948–2957, https://doi.org/10.2337/db11-0300

40 Znoiko, S.L., Rohrer, B., Lu, K., Lohr, H.R., Crouch, R.K. and Ma, J.X. (2005) Downregulation of cone-specific gene expression and degeneration of cone photoreceptors in the Rpe65-/- mouse at early ages. *Invest. Ophthalmol. Vis. Sci.* **46**, 1473–1479, https://doi.org/10.1167/iovs.04-0653

41 Di Pierdomenico, J., García-Ayuso, D., Pinilla, I., Cuenca, N., Vidal-Sanz, M., Agudo-Barriuso, M. et al. (2017) Early events in retinal degeneration caused by rhodopsin mutation or pigment epithelium malfunction: differences and similarities. *Front. Neuroanat.* **11**, 14, https://doi.org/10.3389/fnana.2017.00014

42 Luan, Y.Y. and Yao, Y.M. (2018) The clinical significance and potential role of c-reactive protein in chronic inflammatory and neurodegenerative diseases. *Front. Immunol.* **9**, 1302, https://doi.org/10.3389/fimmu.2018.01302

43 Harmse, B. and Kruger, H.S. (2010) Significant differences between serum CRP levels in children in different categories of physical activity: the PLAY study. *Cardiovasc. J. Africa* **21**, 316–322

44 Laursen, J.V., Hoffmann, S.S., Green, A., Nybo, M., Sjolie, A.K. and Grauslund, J. (2013) Associations between diabetic retinopathy and plasma levels of high-sensitive C-reactive protein or von Willebrand factor in long-term type 1 diabetic patients. *Curr. Eye Res.* **38**, 174–179, https://doi.org/10.3109/02713683.2012.713153

45 Rassouli, M., Sambasivam, H., Azadi, P., Dell, A., Morris, H.R., Nagpurkar, A. et al. (1992) Derivation of the amino acid sequence of rat C-reactive protein from cDNA cloning with additional studies on the nature of its dimeric component. *J. Biol. Chem.* **267**, 2947–2954

46 de Beer, F.C., Baltz, M.L., Munn, E.A., Feinstein, A., Taylor, J., Bruton, C. et al. (1982) Isolation and characterization of C-reactive protein and serum amyloid P component in the rat. *Immunology* **45**, 55–70

47 Griselli, M., Herbert, J., Hutchinson, W.L., Taylor, K.M., Sohail, M., Krausz, T. et al. (1999) C-reactive protein and complement are important mediators of tissue damage in acute myocardial infarction. *J. Exp. Med.* **190**, 1733–1740, https://doi.org/10.1084/jem.190.12.1733

48 Cogan, D.G., Toussaint, D. and Kuwabara, T. (1961) Retinal vascular patterns. IV. Diabetic retinopathy. *Arch. Ophthalmol.* **66**, 366–378, https://doi.org/10.1001/archopht.1961.00960010368014

49 Wong, T.Y., Cheung, C.M., Larsen, M., Sharma, S. and Simo, R. (2016) Diabetic retinopathy. *Nat. Rev. Dis. Primers* **2**, 16012, https://doi.org/10.1038/nrdp.2016.12

50 Blaschke, F., Bruemmer, D., Yin, F., Takata, Y., Wang, W., Fishbein, M.C. et al. (2004) C-reactive protein induces apoptosis in human coronary vascular smooth muscle cells. *Circulation* **110**, 579–587, https://doi.org/10.1161/01.CIR.0000136999.77584.A2

51 Chen, J., Gu, Z., Wu, M., Yang, Y., Zhang, J., Ou, J. et al. (2016) C-reactive protein can upregulate VEGF expression to promote ADSC-induced angiogenesis by activating HIF-1alpha via CD64/PI3k/Akt and MAPK/ERK signaling pathways. *Stem Cell Res. Ther.* **7**, 114

52 Verma, S., Wang, C.H., Li, S.H., Dumont, A.S., Fedak, P.W., Badiwala, M.V. et al. (2002) A self-fulfilling prophecy: C-reactive protein attenuates nitric oxide production and inhibits angiogenesis. *Circulation* **106**, 913–919, https://doi.org/10.1161/01.CIR.0000029802.88087.5E

53 Schneeweis, C., Grafe, M., Bungenstock, A., Spencer-Hansch, C., Fleck, E. and Goetze, S. (2010) Chronic CRP-exposure inhibits VEGF-induced endothelial cell migration. *J. Atheroscler. Thromb.* **17**, 203–212, https://doi.org/10.5551/jat.3004

54 Stefansson, E. (2006) Ocular oxygenation and the treatment of diabetic retinopathy. *Surv. Ophthalmol.* **51**, 364–380, https://doi.org/10.1016/j.survophthal.2006.04.005

55 Bharadwaj, D., Stein, M.P., Volzer, M., Mold, C. and Du Clos, T.W. (1999) The major receptor for C-reactive protein on leukocytes is fcgamma receptor II. *J. Exp. Med.* **190**, 585–590, https://doi.org/10.1084/jem.190.4.585

56 Devaraj, S., Du Clos, T.W. and Jialal, I. (2005) Binding and internalization of C-reactive protein by Fcgamma receptors on human aortic endothelial cells mediates biological effects. *Arterioscler. Thromb. Vasc. Biol.* **25**, 1359–1363, https://doi.org/10.1161/01.ATV.0000168573.10844.ae

57 Liang, Y.J., Shyu, K.G., Wang, B.W. and Lai, L.P. (2006) C-reactive protein activates the nuclear factor-kappaB pathway and induces vascular cell adhesion molecule-1 expression through CD32 in human umbilical vein endothelial cells and aortic endothelial cells. *J. Mol. Cell Cardiol.* **40**, 412–420, https://doi.org/10.1016/j.yjmcc.2005.12.008

58 Banki, Z., Kacani, L., Mullauer, B., Wilflingseder, D., Obermoser, G., Niederegger, H. et al. (2003) Cross-linking of CD32 induces maturation of human monocyte-derived dendritic cells via NF-kappa B signaling pathway. *J. Immunol.* **170**, 3963–3970, https://doi.org/10.4049/jimmunol.170.8.3963

59 Mezzano, S., Aros, C., Droguett, A., Burgos, M.E., Ardiles, L., Flores, C. et al. (2004) NF-kappaB activation and overexpression of regulated genes in human diabetic nephropathy. *Nephrology Dialysis Transplant.* **19**, 2505–2512, https://doi.org/10.1093/ndt/gfh207

60 Mold, C. and Du Clos, T.W. (2006) C-reactive protein increases cytokine responses to *Streptococcus pneumoniae* through interactions with Fc gamma receptors. *J. Immunol.* **176**, 7598–7604, https://doi.org/10.4049/jimmunol.176.12.7598

61 Chen, Q. and Ma, J.X. (2017) Canonical Wnt signaling in diabetic retinopathy. *Vision Res.* **139**, 47–58, https://doi.org/10.1016/j.visres.2017.02.007